

Membranes of Poly(phenylene oxide) and Its Copolymers: Synthesis, Characterization, and Application in Recovery of Propylene from a Refinery Off-Gas Mixture

Susheela Bai Gajbhiye

Department of Engineering Chemistry, College of Engineering, Andhra University, Visakhapatnam 530 003, India
Correspondence to: S. B. Gajbhiye (E-mail: yahuinsb@yahoo.co.in)

ABSTRACT: Copolymers of 2,6-dimethyl-phenol (DMP) and 2,6-diphenyl-phenol (DPP) were synthesized in the initial molar ratio of 100 : 0 (S(PPO)), 90 : 10 (Co-A), 75 : 25 (Co-B), 65 : 35 (Co-C), and 0 : 100 (PDPPO). Dense membranes of 30 μm thickness were tested for single gas permeation and binary mixture separation of 55:45 (in mol %) propylene-propane at $30^\circ\text{C} \pm 2^\circ\text{C}$. Their performance was ultimately examined in the enrichment of propylene from a refinery off-gas mixture (ROG or also called as absorber tail gas, ATG) having the same composition as the ATG of a fluid catalytic cracking (FCC) unit of HPCL refinery, Visakhapatnam. The mixture contains C_1 – C_5 hydrocarbons and nonhydrocarbons such as CO , CO_2 , H_2 , and N_2 . A detailed permeation study of the hydrocarbon part of ATG revealed that using S(PPO) and Co-A, propylene could be upgraded from ~ 29 mol % (on nonhydrocarbon free basis) to 62.2 and 74.4 mol % with propylene/propane selectivity ratio of 5.99 and 8.45, respectively. The structure of polymers was characterized by Fourier transform infrared (FTIR), proton nuclear magnetic resonance (Proton NMR), viscosity measurements. Scanning electron microscope (SEM), wide angle X-ray diffraction (WAXD), density and fractional free volume measurements were used for studying membrane morphology. Dynamic mechanical thermal analyzer (DMTA) and tensile testing were carried to find glass transition temperature (T_g) and mechanical properties. The relative differences observed in gas permeation of these polymers were correlated with the physical properties measured. S(PPO) and Co-A were identified as potential materials for the upgradation of propylene from refinery off-gas streams. © 2012 Wiley Periodicals, Inc. *J. Appl. Polym. Sci.* 000: 000–000, 2012

KEYWORDS: gas separation; propylene-propane; refinery off-gas; recovery; poly(phenylene oxides)

Received 6 September 2011; accepted 18 February 2012; published online

DOI: 10.1002/app.37548

INTRODUCTION

Refinery off-gas (ROG) is the most significant source of wasted fuel generated from FCC and other operations. It is also the primary source of atmospheric emissions from oil and gas operations. Most refinery off-gas streams contain a major percentage (30–80%) of hydrogen gas mixed with smaller proportions of light hydrocarbons (C_1 – C_5) of olefinic and paraffinic nature. The processing required to separate the useful olefins from fuel grade paraffins of ROG is difficult and expensive, so this valuable material is burned in the refineries. Because ROG also contain trace components of heavy sulfur compounds, ammonia, nitriles, chlorides, mercury, arsenic, oxygen, acetylene in addition to acid gases H_2S , CO_2 , and COS , burning of these streams as fuel or release into the air, contribute to environmental impacts both locally and globally by emissions of carbon particulate matter and green house gases. These gases cause atmospheric ozone depletion, global warming, climate changes,

ecological imbalances, loss of human health and property. From an economic analysis done by Baker, H_2 and olefins, such as ethylene and propylene, are more than three times valuable if recovered as chemical feed stock rather than burned as fuel. Also, C_3 paraffin is 1.8 times more valuable if separated as LPG.¹ Hence, alternative technologies to recover valuable components from refinery off-gases need to be prompted to minimize the emission levels. Researchers envisage membrane-based gas separations and component recoveries as potential alternative technologies.

However, the industrial implementation of such alternative technologies for separating olefin/paraffin gas mixtures, of small and similar size is still a great challenge. It requires consideration of several crucial factors viz. (i) the selection of the right membrane material capable of differentiating between two gases of similar molecular sizes, (ii) membranes having high flux and selectivities at the same time, (iii) low cost of membrane production, (iv)

© 2012 Wiley Periodicals, Inc.

membranes that have good stability under stringent operating conditions, and (v) exhibit good mechanical strength.

From the literary citations glassy polymers have been used in practice for the separation of olefins and paraffins as well as for the separation of aromatic, alicyclic, and aliphatic hydrocarbons. Rubbery polymers have been used, in general, for gas/vapor separation processes and in pervaporation separation of hydrocarbon vapors from their aqueous solutions.² Chemically modified membranes in the form of immobilized liquid membranes, composite inorganic-polymer membranes, zeolite membranes and carbon membranes have been experimented and reported to exhibit significantly huge improvements in the propylene permeance and separation factors (Table I).^{3–11} However, when applied on a large scale these modified membranes are expensive and unstable. Consequently the scope for polymer-based membranes widens. Polymer membranes can serve good stability under the operating conditions and also lower the cost of production. In addition, polymers can also be chemically modified as per the property required for specific applications. Thus polymer-based membranes are supposed to be versatile in all respects. Poly(2,6-dimethyl-1,4-phenylene oxide) (PPO) can be listed as one of such polymers due to its high glass transition temperature ($T_g = 210^\circ\text{C}$), high mechanical strength, and excellent hydrolytic stability. Its distinctive but simple structure allows a variety of chemical modifications.

In this regard, the authors have earlier reported their studies on commercially available PPO (C(PPO)) of molecular weight 53,000, in the separation of propylene-propane mixtures, indicating better propylene/propane selectivities but with lower net permeabilities and brittleness.¹² C(PPO) incorporated with certain metal ions (<1 wt %), acting as fixed carriers for propylene, exhibited twofold increase in the selective permeation of propylene at $30^\circ\text{C} \pm 2^\circ\text{C}$. A high selectivity of 7.5 with enhanced gas permeabilities has been obtained using these metal incorporated membranes.¹² It was also observed that PPO membranes of varying origin and molecular weights exhibited quite different values of separation factors and gas permeabilities in the separation of these gas mixtures when all other factors affecting gas permeation were kept fixed, namely membrane thickness, polymer solution concentration, casting conditions, feed pressure, and temperature of gas separation. The effect of these factors on gas transport is reported in Refs. 13–16. The molecular weight of a polymer affects several properties of a polymer, such as mechanical properties, thermophysical properties, and the transport properties of its film. Lower molecular weight polymers with molecular weights above that required for entanglement, have relatively unstrained chain packing configuration due to greater number of chain ends per unit volume than high molecular weight polymers.¹⁷ Hence, membranes of the former type of polymers are expected to exhibit relatively greater transport properties and produce useful range of physical and mechanical properties, suitable for specific applications. However this aspect of gas transport by polymers of varying molecular weights needs rigorous studies.

In this article, we report the direct enrichment of propylene, carried out on a bench scale at room temperature, from a multicomponent refinery off-gas (ATG) containing ~ 29 mol %

propylene as the major constituent, by using membranes of low molecular weight polymer poly(2,6-dimethyl-1,4-phenylene oxide) (S(PPO)) and its copolymers prepared in-house. Copolymers of 2,6-dimethyl-phenol (DMP) and 2,6-diphenyl-phenol (DPP) were synthesized in the initial molar ratio of 90 : 10 (Co-A), 75 : 25 (Co-B), 65 : 35 (Co-C), and 0 : 100 (PDPPO). The polymers were characterized by dilute solution intrinsic viscosity, fourier transform infrared (FTIR) spectroscopy, and proton NMR for confirming structure and also for the determination of copolymer composition. Films of these polymers were characterized for T_g by DMTA and for mechanical properties by tensile tester. Their morphology was studied by SEM, WAXD, density measurement, and fractional free volume (FFV) estimation. The observed permeation results are interpreted by structure-property correlations.

EXPERIMENTAL

Materials

The 2,6-dimethyl-phenol (DMP) and dibutyl amine (DBA) from Merck Chemie, Mumbai, 2,6-diphenyl-phenol (DPP) from Aldrich Chem. Co., cuprous bromide catalyst from Lancaster and synthesis grade toluene and chloroform from Ranbaxy were procured. Distilled methanol was used for washing the polymer precipitate. Propylene and propane gases obtained from Bhoruka Gas, Bangalore, were found 99.5% pure and were used without further purification. The gas mixture containing ~ 45 mol % propane and ~ 55 mol % propylene was prepared online with the help of multichannel mass flow controllers calibrated with a soap bubble meter. Two mixing vessels were installed in the feed line to ensure the homogeneity of the mixtures (Figure 1). A gas mixture similar in composition to the absorber tail gas (ATG), containing C_1 – C_5 hydrocarbons and other nonhydrocarbons was obtained from Speciality Gas, Mumbai, India. Table II gives the detected composition of only the hydrocarbons present in the multicomponent ATG. The values are reported on a nonhydrocarbon-free basis.¹⁸

Synthesis of the S(PPO) Polymer and Copolymers with DPP

The synthesis of S(PPO) from its DMP monomer was carried out by oxidative coupling method according to the procedure given in literature.¹⁹ DMP was purified by recrystallization with hexane to at least 99.5%. In a three necked flask, oxygen was introduced into a vigorously stirred solution of CuBr and DBA in toluene. Maintaining a molar ratio of CuBr : DBA : DMP equal to 1 : 22 : 77, a 25% solution of DMP in toluene was added over a period of 20 min. The temperature of solution was maintained throughout at 40°C . After 75 min of reaction time and stirring, the reaction mixture was diluted in toluene to 10%. Methanol (5–7 vol.) containing 0.5–1.0% acetic acid was added gradually to precipitate out the PPO polymer as agglomerates which slowly turn into granular powder. The polymer was filtered and washed with methanol, and dried in a vacuum oven at 60°C . PDPPO and copolymers of DMP and DPP with initial molar ratio of 90 : 10 (Co-A), 75 : 25 (Co-B), and 65 : 35 (Co-C) were also prepared in the same manner. The yield is over 95%.

Fabrication of Dense Films

Films of the polymers synthesized were obtained by solution casting at $30^\circ\text{C} \pm 2^\circ\text{C}$. A 12 wt % solution of the polymers was

Table 1. Separation Performance of Different Membranes for Propylene and Propane

Membrane type	Name of membrane used	Propylene permeance (Barrer)	Separation factor	Reference
Glassy polymers	Cellulose acetate	15.2	2.6	2
	Polyimide	0.8	27	3
	Polyphenylene oxide	2.3	9.1	3
Rubbery polymers	Polydimethyl siloxane	6600	1.1	2
	Ethyl cellulose	52	3.3	4
Facilitated transport membranes: (a) solid polymer electrolyte membrane	PAAM/AgBF ₄ (67mol % Ag ⁺)		170	5
	PVDF/20 wt % aqueous AgNO ₃ , 120 kPa	Flux = 1.46×10^{-4} mol m ⁻² s ⁻¹ at 70 : 30 vol % feed composition	270 (at 50 : 50 mol % feed mixture)	6
Facilitated transport membranes: (b) immobilized liquid membranes	PVDF/20 wt % aqueous AgNO ₃ , 120 kPa		474 (at 30 : 70 mol % feed mixture)	6
	Gas-liquid membrane contactor system containing AgBF ₄ as absorption liquid		250 (at 80 : 20 mol % feed mixture)	7
	TEG and its mixture with AgBF ₄ and AgNO ₃ . Highest separation factor of 110 with TEG/AgBF ₄ liq membrane		110	8
Carbon membranes	Poly-azide/PAEK pyrolyzed at 550°C	48	44	9
	PDMS coated membranes on PSF support coupled with silica nanoparticles	42	8.5	10
Zeolite membrane	Faujasite type zeolite membranes on porous alpha- alumina supports are propylene permeable		13.7 (100°C) and 28 (35°C)	11

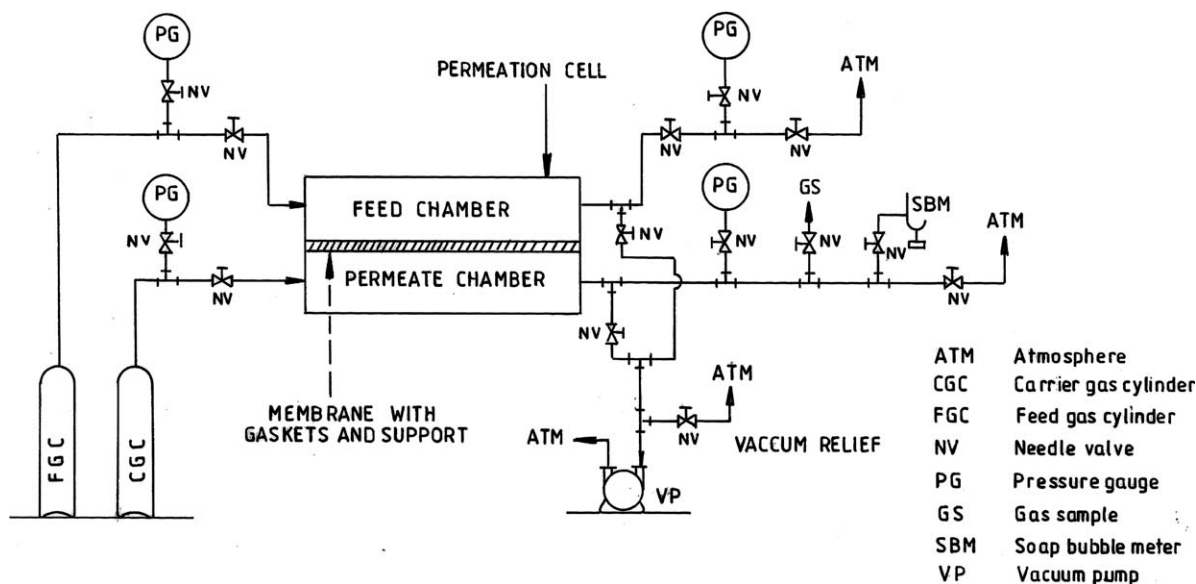


Figure 1. Manifold used for gas permeation studies.

prepared in chloroform solvent (AR Grade) which was immediately cast on a glass plate in an enclosed chamber to avoid free air contact. The films of uniform thickness were obtained which were then vacuum dried for 6 h.

Polymer Characterization

FTIR Analysis. FTIR spectroscopy was performed on the chloroform solution cast thin films (30- μm thick) of the all synthesized polymer and which were vacuum dried. Shimadzu FTIR instrument was used for scanning the films, at ambient temperature, at the rate of 400 sweeps per second.

Proton NMR. Gemini 200 MHz machine was used to determine the structure of the synthesized copolymer and the homopolymer (solvent CDCl_3).

Intrinsic Viscosity. The intrinsic viscosity of the dilute polymer solutions in toluene was calculated from the flow time measure-

ments, using a Schott Gerate Dilute Solution Viscometer (Germany) with an automatic recorder at 25°C. The required constants were taken from literature.²⁰

WAXD. Siemens D5000 powder X-ray diffractometer was used, to find the effective spacing between intersegmental polymer chains, characterized by d_{eff} of the samples. X-rays of wavelength 1.5406 Å were generated using Cu K α source. The 2θ value was varied from 0° to 65°. The powder samples were partially wetted in toluene vapor (yet retaining their powdery nature) and then used for diffraction studies to reduce anisotropy of the diffracting planes. The characteristic peaks (in 2θ units) for PPO, copolymers and PDPPO are computed and indicated by computer which are shown against the corresponding peaks. To arrive at a single averaged 2θ values for the copolymers, method reported in Ref. 21 was followed. From the two significant characteristic peaks (corresponding to DMP and DPP units) a smooth halo was drawn around them using polynomial curve fitting of sixth degree. The averaged 2θ value was noted from its maxima and the same is indicated in brackets in the WAXD pattern. Bragg's equation of first order is used to calculate the d_{eff} from 2θ values of the polymers and is reported with an accuracy of ± 0.01 .

Tensile Test. The mechanical properties of the polymer films cut as rectangular pieces of uniform dimensions were determined using Universal tensile testing machine (UTM), AGS-10 KNG, Shimadzu, at the deformation rate of 5 mm min^{-1} , keeping a gage length of 7 cm. The measured mechanical properties correspond to an average value calculated on five films of each polymer sample, with an error margin <1.5%.

Density. The density of the polymer membranes was measured, by floatation method at 30°C \pm 2°C using mixtures of ethylene glycol and DMF solvents. Additionally, the density was measured by two more methods to ascertain the accuracy of the values. In the second method, weight of 100 mL polymer solutions

Table II. Detected Composition of the Hydrocarbons Present in ATG Mixture

Hydrocarbon component	Composition (mol %)
Methane	7.0–10.0
Ethane + ethylene	20.0–22.0
Propane	18.0–21.0
Propylene	28.5–31.0
Isobutane	4.0–5.5
1-Butene	5.0–6.5
N-Butane	1.5–2.5
Trans-2-Butene	1.5–2.5
Cis-2-Butene	1.5–2.5
Isopentene	1.0–2.0
1-Pentene	0.4–0.7
n-Pentane	0.5–1.5

(12 wt % in chloroform) was measured in 100 mL pycnometer. As a third method, hydrostatic weighing was used for the determination of film densities. Isopropanol was chosen as a liquid with known density. It is also a nonsolvent for the polymers studied and has a low diffusion coefficient. It allows neglecting the effects of absorption and swelling on density measurements. The density was calculated using the formula $\rho = [W_a/(W_a - W_l)] \rho_b$ where ρ is the density of the film sample, W_a the weight of the sample in air, W_l is the weight of the sample in liquid and ρ_l is the density of the liquid at the temperature of measurement.²² The density was measured using above methods by taking five reading for each polymer sample. The density values are reported with an error margin of <1%.

Fractional Free Volume. FFV values of the polymers were estimated using their density (ρ) values. FFV is defined as $FFV = V_f/V_{sp}$, where V_f is free volume and $V_{sp} = 1/\rho$ is the specific volume of the polymer. According to Bondi, V_f can be estimated as $V_f = V_{sp} - 1.3 V_w$. V_w is the vander Waal's volume of the repeat unit of the polymer and it is calculated using group contribution method.²³ Statistical weights of both the comonomers were taken into account in these calculations. The FFV values have been reported with an accuracy ± 0.005 .

DMTA. Dynamic mechanical thermal analyzer DMTA model IV, Rheometric Scientific, USA, was used to determine the T_g of the polymers from the temperature corresponding to the maximum $\tan \delta$ value. The temperature range of 25–350°C was scanned at the rate of 5°C min⁻¹ and a strain rate of 0.75% at a frequency of 1.5 Hz, in compression mode. Discs of 16 mm diameter were prepared from the samples of the measurement. The T_g reported corresponds to maximum of $\tan \delta$ values (computerized data given by the instrument) for the samples.

SEM. Scanning electron microscopy, Hitachi-S 520 model, was used for studying the surface morphology of the polymers. Before analyzing, the film sample was coated with a thin layer of gold. The images reported have a magnification of $\times 1500$ with a scale of 20 μm .

Gas Permeation Studies on the In-House Built Gas—Separation Manifold

A schematic of the experimental set-up used for gas permeation studies is shown in Figure 1. The experiments were conducted at a temperature of 30°C \pm 2°C with pure gases as well as mixtures of propane (44.90 mol %), propylene (54.95 mol %), and C₂ hydrocarbon (0.15 mol %) as detected by gas chromatography (GC). Mixtures were tested on a manifold containing two feed lines connected to two mixing chambers.¹² Membranes fabricated from S(PPO), Co-A and Co-B could be tested while that of Co-C and PDPPPO could not be evaluated due to leakage and membrane failure upon application of pressure.

Initially, the membrane film, supported on a porous viscose with the help of rubber gaskets, was laid over a perforated steel plate located half way between the feed and permeate chambers in the test cell. The feed and permeate lines were initially evacuated and then the feed gas at a constant feed pressure of 3×10^5 Pa was introduced into the feed chamber. A precision needle valve in the feed line, as shown in Figure 1, was used to main-

Table III. Pure and Binary Mixture Gas Permeability Results

Polymer	Permeability (P) (Barrer)		Selectivity α_{mix} (α_{ideal})
	Propylene	Propane	
S (PPO)	9.00 (9.23)	1.67 (1.69)	5.38 (5.46)
Co-A	10.10 (10.46)	1.39 (1.41)	7.26 (7.42)
Co-B	2.49 (2.84)	0.18 (0.19)	13.83 (14.95)

The values in brackets correspond to pure gas permeabilities.

tain constant feed pressure throughout the experiment. The permeate gas was collected under a pressure differential of 2×10^5 Pa, in SS 316 gas sampling bombs, from the lower chamber of the test cell. Nitrogen at a controlled flow rate was used as the carrier gas.

Pure and Mixture Gas Permeation Study

Only steady state samples were collected. The feed and permeate samples were analyzed with a gas chromatograph Shimadzu 17A Model, Japan, using the same conditions and columns used in our earlier work.¹² The respective pure and mixture gas permeabilities (P) and selectivities (α) were calculated and are reported in Table III. The values reported are averaged over all observations with an error margin <3.0%.

ATG Permeation Study

Experiments with the synthesized ATG feed were conducted on the same manifold. GC analysis of the feed and permeate mixtures was done by using two types of columns: (1) a dual column (CTR), consisting of a combination of two columns—molecular sieves 13 Å and porapak-Q, provided with thermal conductivity conductor (TCD), was used for estimating the nonhydrocarbons.¹⁸ This column could not be used for detecting hydrocarbons. (2) Independently, a separate 23% SP-1700P AW column was used with field ionization indicator (FID) for estimation of hydrocarbons on a nonhydrocarbon (H₂, N₂, CO, CO₂) free basis. The feed mixture for the current study was found to contain 29–31 mol % propylene and 18–21 mol % propane as the major components and other C₁–C₅ hydrocarbons as the minor components. A feed pressure of 3×10^5 Pa and a stage cut of 0.025–0.028 was maintained. The values reported are averaged over all observations with an error margin <3.4%.

Calculations

- From the characteristics of the membrane, propylene/propane ideal selectivity (α_{ideal}) and selectivity for binary mixture (α_{mix}), were calculated as reported earlier.¹²
- Permeability coefficient (P) is calculated as (flux \times thickness)/partial pressure difference.
- For ATG multicomponent mixture, stage cut is calculated as flow rate of permeate/flow rate of feed, or fraction of feed stream allowed to permeate through the membrane. The selectivity was calculated with respect to the slowest permeating component i.e., *n*-pentane (*n*-C₅H₁₂), where permeability of *n*-pentane (or *n*-C₅H₁₂) is $P(n\text{-C}_5\text{H}_{12}) = 0.6$ Barrers. Therefore, we report the selectivity ratio as the selectivity for C₃H₆/C₃H₈ here.

$$\text{Selectivity ratio (C}_3\text{H}_6/\text{C}_3\text{H}_8) = \{P(\text{C}_3\text{H}_6)/P(n\text{-C}_5\text{H}_{12})\} / \{P(\text{C}_3\text{H}_8)/P(n\text{-C}_5\text{H}_{12})\}$$

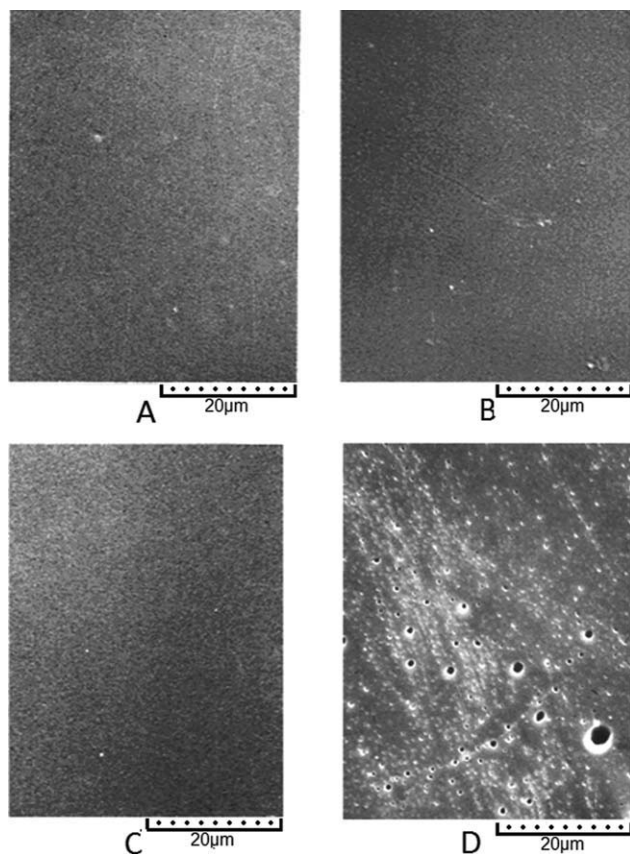


Figure 2. SEM micrographs of (A) S(PPO), (B) Co-A, (C) Co-B, and (D) Co-C (magnification $\times 1500$).

The values reported are averaged over all observations with an error margin $< 3.4\%$.

RESULTS AND DISCUSSION

It was observed that good quality dense membranes of the synthesized polymers could be obtained in an enclosed chamber under normal room temperature ($30^{\circ}\text{C} \pm 2^{\circ}\text{C}$) and atmospheric pressures, unlike those of C(PPO). Films of S(PPO), Co-A, and Co-B appeared transparent showing homogeneous and uniform surface morphology in SEM photographs (Figure 2). Films of Co-C were hazy having some distinct surface irregularities (microvoids) distributed uniformly throughout the film in the SEM micrograph.

FTIR Spectra

Figure 3 shows FTIR spectra of PPO and copolymers Co-A, Co-B, and Co-C.

PPO. The characteristic aromatic ring —C—H stretching bands occur at 3036 and 2954 cm^{-1} . The methyl group stretching gives sharp peaks at 2922 and 2860 cm^{-1} . Whereas absorptions at 1306 and 1022 cm^{-1} are the C—O—C (ether) group stretching vibrations and their characteristic deformations occur at 1185 – 1200 cm^{-1} .

Copolymers. The FTIR spectra of the copolymers are very much similar to that of the PPO, except for the presence of

extra 2,6-diphenyl group substitutions. Aromatic C—H asymmetric stretching band at 3036 cm^{-1} was found proportionately split into two distinct peaks as 3036 and 3055 cm^{-1} with the increasing concentration of the 2,6-diphenyl groups. These peaks indicate the presence of substituted phenyls and backbone phenyl groups, respectively.

Proton NMR Spectra

Figure 4 represents proton NMR of PPO and of copolymer Co-A. For PPO a six proton singlet corresponding to two equivalent methyl protons is observed at δ of 2.1 ppm and the remaining two equivalent aromatic protons give a two proton singlet absorption at 6.4 ppm. PDPPO has peaks at 6.3 ppm (two proton, Ar-H, labeled “b”), 6.9 ppm (two proton, Ar-H)

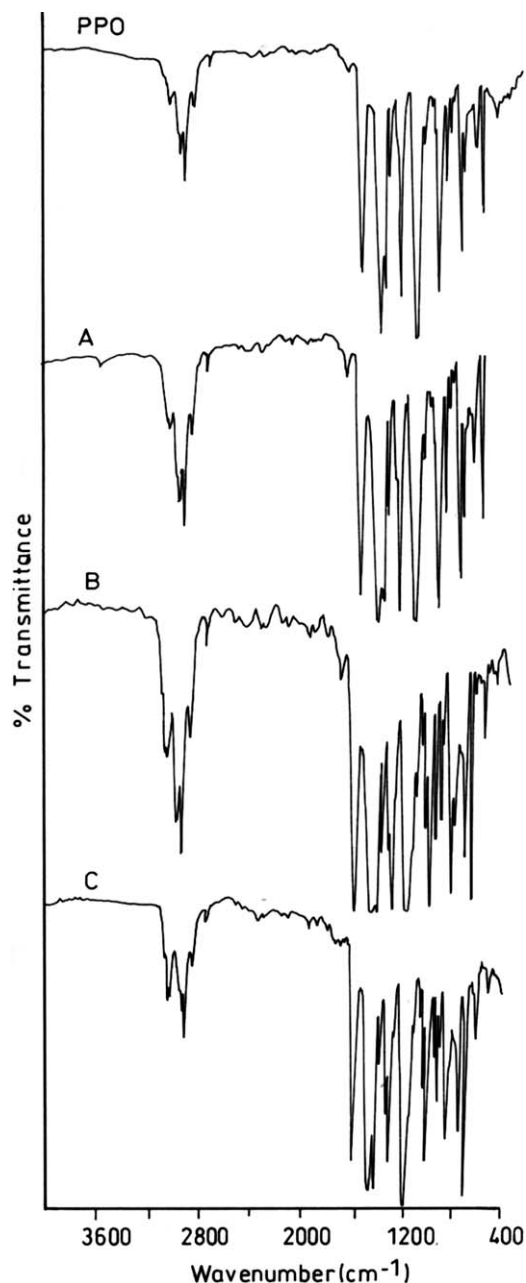


Figure 3. FTIR spectra of S(PPO), (A) Co-A, (B) Co-B, and (C) Co-C.

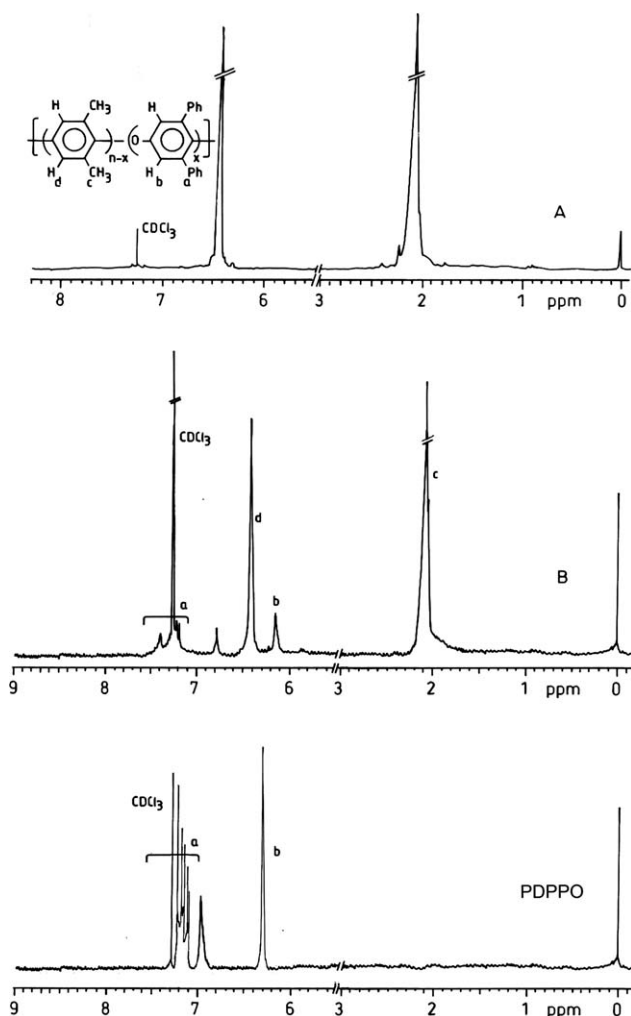


Figure 4. Proton NMR spectra of (A) S(PPO) (B) Co-A, and (C) PDPPO.

and at 7.1–7.3 ppm (multiplet aromatic proton, labeled “a”). In the case of copolymers, on comparison with PPO and PDPPO, we find that there are two sets of equivalent protons existing in two different chemical environments. At $\delta = 2.0\text{--}2.2$ ppm (singlet $-\text{CH}_3$ protons labeled “c”), at $\delta = 6.15$ ppm (Ar-H labeled “b”), at $\delta = 6.43$ ppm (singlet Ar-H labeled “d”) and at $\delta = 6.7\text{--}7.5$ ppm (multiplet aromatic protons labeled “a”) are observed.

Calculation of Copolymer Ratio

The final copolymer ratio can be determined using the quantitative analysis of FTIR and NMR spectra.²⁴ From FTIR data a calibration graph was plotted for a series of blends of PPO and PDPPO mixed in various molar percentages. A plot was drawn taking the ratio of absorbance at $2860\text{--}3100\text{ cm}^{-1}$ to 1200 cm^{-1} versus the mol % of DPP in the blend. By interpolation the copolymer composition was determined (with an error margin $<0.5\%$). However at higher DPP mol %, scatter in the plot was observed. Hence, copolymer composition was also calculated using proton NMR method. Accurate results with (error margin $<0.3\%$) could be obtained using either the peak heights or peak areas even at higher DPP mol %. The ratio of peak areas at $\delta =$

Table IV. Copolymer Composition (Calculated as DPP mol %) Determined Using Quantitative FTIR and Proton NMR Analysis

Polymer	Initial monomer ratio (mol %)		Calculated comonomer (DPP) concentration (mol %)		
	DMP	DPP	IR	NMR	
				Average	wt %
Co-A	90	10	6.25	8.83	15.1
Co-B	75	25	13.20	14.53	25.8
Co-C	65	35	-	23.68	38.2

6.15 ppm to 2.0–2.2 ppm and the ratio of peaks at $\delta = 6.43$ ppm to $\delta = 2.0\text{--}2.2$ ppm were considered for determining DPP mol % in the copolymers. An average of the two ratios obtained is reported as the NMR average DPP mol %. The final values of copolymer composition calculated by both these methods are given in Table IV. Values reported for DPP mol % calculated by IR is within error margin $<0.5\%$ and those calculated by NMR is within error margin $<0.3\%$. These were found to be lower than the initial molar ratio of the monomers taken.

Study of Physical Properties

The measured physical properties are listed in Table V. The viscosity average molecular weight measured from dilute solution intrinsic viscosity measurement was found to be 29,500 for S(PPO) and 53,000 for C(PPO). The intrinsic viscosity of the copolymers (in dL g^{-1}) at 25°C were found to be 0.310, 0.286, 0.292, and 0.248 dL g^{-1} , with increasing DPP (i.e., S(PPO), Co-A, Co-B, and Co-C, respectively). Commercial C(PPO) has intrinsic viscosity 0.455 dL g^{-1} and PDPPO has an intrinsic viscosity of 0.241 dL g^{-1} .

The Glass Transition Temperature (T_g). T_g for S(PPO) was found to be 235°C (Table V), which is lower than C(PPO) by 5°C . It may be noted that the T_g values reported here are obtained by dynamic methods, which are always higher by about 20°C compared to thermally obtained values.²⁰ With the increasing content of DPP in the copolymers, the T_g was found to increase. However, T_g of Co-A was 235°C , same as that of S(PPO). This probably implies that Co-A with low DPP content, is as flexible as that of S(PPO). The increase in T_g values for Co-B and Co-C is due to the presence of higher proportions of rigid phenyl side groups of DPP, which reduce the chain flexibility of the main chain. Higher the chain stiffness of polymer segments, lesser is the gas diffusion through their films.

Table V. Physical and Mechanical Properties of S(PPO) and Copolymers

Polymer	Intrinsic viscosity (dL g^{-1})	T_g ($^\circ\text{C}$)	Tensile properties		
			Tensile strength (MPa)	Elongation at break (%)	Elastic modulus (MPa)
S(PPO)	0.310	235	39	16	21
Co-A	0.286	235	28	16	15
Co-B	0.292	262	32	5	9
Co-C	0.248	299	25	4	7

Table VI. WAXD, Density, and Fractional Free Volume Results of S(PPO) and Copolymers

Polymer	Diffraction angle (2θ)	d_{eff} (Å) (^a average d_{eff})	Density (kg m^{-3})	Fractional-free volume
C(PPO)	13.49	6.56	1060	0.198
S(PPO)	13.27	6.67	1058	0.199
Co-A	14.50	6.10 ^a	1079	0.186
Co-B	15.75	5.62 ^a	1128	0.151
Co-C	16.50	5.36 ^a	1142	0.144
PDPPO	19.80	4.48	1223	0.110

Tensile Properties. From the tensile load-displacement behavior, S(PPO), Co-A, Co-B, and Co-C were found to exhibit typical plastic behavior with the brittle fracture becoming more prominent with increasing DPP. Interestingly, Co-A was found to have undergone a relatively extensive elongation (16%) before tensile failure, reflecting a larger area under its curve compared to other copolymers (Table V). This implies that Co-A is relatively more elastic and tougher than the rest of the copolymers. Thus, the tensile properties and glass transition temperature results indicate that the introduction of small proportion of DPP groups (as in Co-A) has not altered the chain flexibility much when compared to S(PPO). However, with further additions of diphenyl groups the chain flexibility reduces in Co-B and Co-C making them reach break point earlier.

Density. The measured density values were found to increase with increasing DPP content except for Co-A which showed only a small increase (Table VI).

FFV Values. The FFV values were estimated using measured density values for the various polymers (Table VI). These were found to decrease with increasing DPP content in the copolymers. Such decrease in FFV for phenylene oxide polymers with increasing DPP content was also reported by Ilinich.^{2,25}

WAXD. Wide Angle X-ray techniques provide average d -spacings (also referred as d_{eff}) of a polymer matrix. A lower average d_{eff} corresponds to a lower average intermolecular distance, allowing less passage of gas molecules and vice versa. On comparing the diffraction patterns of S(PPO), copolymers and PDPPO, from Figure 5, the following observations were made: (1) S(PPO) shows a definite main peak at $2\theta = 13.27^\circ$ (corresponding to DMP units) with d_{eff} of 6.67 Å; (2) PDPPO has a definite main peak at $2\theta = 19.8^\circ$ (corresponding to DPP units) with $d_{\text{eff}} = 4.48$ Å. (Other researchers report PDPPO having a peak around 2θ around 20° ²¹; and (3) Copolymers exhibit a main peak around $2\theta = 13.5^\circ$ – 15.5° (corresponding to DMP units) and a second peak emerging at 2θ value of around 20° – 21° (corresponding to DPP units) with d_{eff} around 4.22–4.44 Å. Further, the intensity of this second peak relative to the main peak is found to increase with the DPP content. Interpretation of the WAXD spectra for copolymer is less straightforward since all the copolymers appear to exhibit almost close d_{eff} values, although gas permeabilities vary over a larger factor.²⁶ There-

fore, in order to interpret the permeability results for copolymers, we have to arrive at a single average d_{eff} value by considering both the peaks. The averaged d_{eff} of the copolymers (given in Table VI) are calculated as explained in WAXD section. Figure 5 clearly shows the 2θ values of the two characteristic maxima separately and the averaged 2θ values in brackets for the copolymers. We find a decreasing trend in the average d_{eff} value with increasing DPP content of copolymers, which is also supported by the decrease in the calculated FFV values (Table VI).

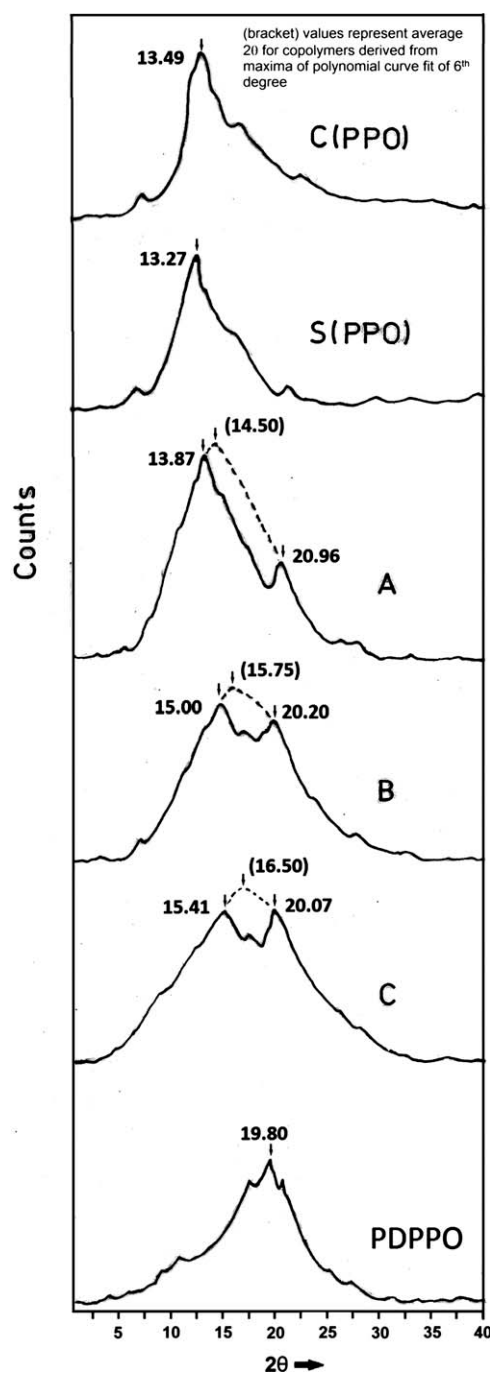
**Figure 5.** WAXD patterns of C(PPO), S(PPO), (A) Co-A, (B) Co-B, (C) Co-C and PDPPO.

Table VII. Permeation Results for S(PPO) and Copolymers on ATG Mixture

Polymer	Permeate composition (mol %)		Permeability (Barrer)		Selectivity propylene/propane
	Propylene	Propane	Propylene	Propane	
S(PPO)	62.2	4.00	5.14	0.86	5.99
Co-A	74.4	4.38	5.99	0.71	8.45
Co-B	70.0	6.00	1.25	0.08	15.26
Co-C	Could not be evaluated				

This means that the polymer intersegmental spacing is decreasing accordingly. This could be attributed to the reason that addition of two rigid pendant phenyl groups (in the form of DPP) onto the polymer backbone in the copolymers, apparently offers steric effects by occupying more space (when compared to space occupied by two methyl groups of DMP, in PPO), resulting in decreased free volume. Thus the membrane acts like a sieve to the permeating gas molecules, whose sieving effect increases with increasing DPP content on moving from S(PPO) to copolymers. As a result low gas permeation in the copolymers is observed.

Experimental Gas Permeation Studies

Pure and Binary Mixture Gas Permeation Studies. S(PPO) and its copolymers were tested for permeation of pure propylene and propane gases as well as their binary mixtures at room temperature, whose results are given in Table III. Co-C and PDPPO showed a tendency to crack immediately upon application of the feed pressure.

S(PPO) Membranes. S(PPO) exhibited an ideal selectivity of 5.46 for propylene/propane with propylene permeability of 9.23 Barrers. From our earlier studies, C(PPO) of molecular weight 53,000 was found to have relatively lower selectivity (3.5) and low flux values.¹² Thus compared to C(PPO) membrane, the permeability and selectivity values for propylene with respect to propane are found to be higher for S(PPO) membrane, which was cast and tested under similar conditions. The reason behind this difference requires further investigation.

Copolymer Membranes. In the case of membranes of copolymers, compared to S(PPO), the propylene/propane selectivity (measured from single as well as binary gas permeability tests) was found to increase from 7.42 to 14.95 with increasing concentrations of DPP, whereas the permeability exhibited a different trend. For Co-A, propylene permeability increased to 10.46 Barrers, while with further increase in DPP content, it decreased to 2.84 Barrers. Our observation with respect to the trend in selectivity is similar to that reported by Ilinich et al.^{27,28} However, the trends in permeability differed. Their reported values of permeability for propylene decreased with increasing concentration of DPP at 50°C. Their reports also indicate high propylene/propane selectivities and formation of good film upto 25 mol % of DPP. In contrast, we obtained poor quality films with Co-C under our polymerization and experimental conditions. As pointed earlier that there can be several factors which influence polymer permeation as well as mechanical properties. As no

data is provided about any of these factors, the results cannot be compared.

Structure and Gas Permeation Property Correlations. The changes in gas permeation, observed in copolymers, with varying DPP mol % can be explained with the help of similar trends observed in the T_g , % elongation at break, FFV and d_{eff} values. Compared to S(PPO), Co-A shows the following changes in physical structure: (i) chain stiffness remains the same (T_g same as S(PPO)), (ii) polymer exhibits same elasticity (from % elongation at break), (iii) intersegmental spacing and polymer free volume only slightly reduced (FFV and d_{eff} deduced from WAXD), (iv) incorporation of a small amount of DPP increases the selective propylene solubility by small amount, perhaps due to increase in the $\pi-e^-$ interactions between the greater number of aromatic groups in polymer and the propylene gas molecules. The first two factors help in enhancing diffusivity of both the gases, but factor (iii) helps to certain extent the selective sieving of the smaller sized propylene gas to diffuse through it retaining the larger sized propane gas, and factor (iv) selectively enhances diffusivity of the more interacting propylene gas in comparison to propane. Thus, selective permeability of propylene is improved for Co-A compared to S(PPO).

In the case of Co-B, compared to S(PPO) and Co-A, the following changes in physical structure occur (i) segmental mobility is reduced (higher T_g) (ii) chains are more stiff and plastic (tensile property) (iii) increased packing density (reduced d_{eff} from WAXD) and (iv) significantly reduced FFV value. None of these diffusion-controlling factors are favorable for either of the gases to permeate through Co-B membrane due to increase in steric factors by larger amounts of incorporation of DPP groups. This also suggests that the Co-B membrane's sieving-effect has been improved over Co-A, on incorporation of higher amounts of DPP, allowing only the smaller sized propylene molecules to pass through and retaining propane gas to a larger extent. Further, the $\pi-e^-$ interactions between propylene-phenyl groups of Co-B perhaps contribute more to the selective solubility of the propylene gas molecules in membrane, when compared to Co-A and S(PPO). Therefore, we observe enhanced propylene/propane selectivity but not enhanced gas permeability for Co-B membrane.

Thus from the comparative study, among membranes of S(PPO) and copolymers, Co-A and S(PPO) can be suggested as potential candidates in the separation of propylene and propane.

ATG Mixture Gas Permeation Studies. S(PPO) and copolymer samples were tested for propylene recovery with ATG mixture (Table VII). On a nonhydrocarbon free basis, it is observed that propylene permeation is higher for the ATG mixture compared to the binary mixtures. A propylene permeate stream of nearly 62.2 mol % is recovered using S(PPO) which corresponds to permeability of 5.14 Barrers with propylene/propane selectivity of 5.99. In the case of Co-A and Co-B, the propylene/propane selectivity ratio obtained is 8.45 and 15.26 with a propylene permeability of 5.99 and 1.25 Barrers, respectively. There is significant enhancement in permeate concentration of propylene when compared to S(PPO).

The ATG gas permeate concentrations as well as the observed trends in propylene permeability and propylene/propane selectivity for S(PPO), Co-A, and Co-B membranes can be found consistent with those obtained with pure gas permeation and also binary mixture results (Table III). However, the enhanced values of propylene/propane selectivity observed for S(PPO), Co-A, and Co-B with ATG mixture, compared to those obtained with pure gases and binary mixture of propylene and propane, could be due to the following factors:

- a. Diffusion factor—selectivity of a membrane indicates its relative behavior toward the two gases. In the case of pure gases, based on diffusion and membrane–gas interaction factors, the permeation of smaller and better interacting propylene is higher than propane. Therefore the ratio of the permeability of the two gases indicates the ideal behavior of the membrane. In a multicomponent mixture the ideal behavior of the membrane towards the two gases is disturbed by the presence of other gases. It can be attributed to the reason that all the other larger sized gas molecules (other than C₃ gases) cause blocking of the path (called as “blocking effect”),²⁹ consequently reducing the probability of the propane which is relatively larger sized (compared to propylene) and less interacting to pass through the membrane. Thus the propane–membrane interactions and its diffusion is lowered in a multicomponent mixture. Whereas in a binary mixture such blocking effects are very feeble due to which the propane–membrane interactions are equally possible in an equimolar mixture with propylene. Hence the membrane selectivity toward propylene is enhanced in a multicomponent mixture.
- b. Interaction factor—It is reported by us earlier that in binary mixture permeation, the significant pairs of interactions are propylene–membrane, propane–membrane, and propylene–propane. In an equimolar binary feed mixture all these interactions equally become significant. However, in ATG feed mixture there is relatively greater concentrations of the unsaturated reactive propylene molecules (29 mol %) when compared to propane (19 mol %).¹⁸ Hence, propylene–propane and propane–membrane interactions pairs become less significant compared to the more dominant propylene–membrane interactions. As we report here the selectivity of PPO membrane for propylene with respect to propane in the multicomponent ATG mixture, it

is higher than that obtained for pure gases and binary mixtures.

CONCLUSIONS

S(PPO) and copolymers of DMP and DPP in various ratios were synthesized and their dense films were tested for recovery of propylene from ATG refinery-off gas mixture at 30°C ± 2°C. It is found that the copolymer ratio significantly influences the mechanical properties, film formation ability, polymer structure, polymer chain flexibility and gas transport properties (permeability and selectivity). When gas transport properties of membranes of S(PPO) (low molecular weight) of present work, was compared to C(PPO) (high molecular weight), of our earlier studies, S(PPO) produced better permeability (9.23 Barrers), selectivity (5.46) for propylene gas and better film formation property. However this observation needs further investigation to substantiate.

When comparing S(PPO) with the copolymers, permeability was found to initially increase with smaller additions of DPP and then decrease for the next higher additions. However, propylene/propane selectivity increased with increasing DPP concentrations. From characterization studies it was concluded that relatively smaller proportions of DPP in Co-A modifies the structure in a favorable way to enhance propylene permeation selectively, consequently improving propylene permeability and selectivity. While incorporation of higher amounts of diphenyl side groups was found to modify the polymer structure by decreasing the free volume leading to low gas permeabilities.

From the studies on the hydrocarbon part of ATG multicomponent mixture, significant enhancements in permeate concentrations of propylene were observed with copolymers and S(PPO). Co-A and S(PPO) have been identified to exhibit significant propylene permeation, with better propylene/propane selectivities making them potential candidates in the industrial recovery of propylene from refinery off-streams.

ACKNOWLEDGMENTS

This work was carried out with the financial help given by Hindustan Petroleum Corporation Ltd. Visakhapatnam (India). The cooperation extended by FTIR group of the analytical division and the Analytical group of Chemical Engineering Division of IICT, Hyderabad (India), is thankfully acknowledged. The author thankfully acknowledges the support provided by Dr. A.A. Khan and K.N. Jayachandran.

NOMENCLATURE

PPO	2,6-dimethyl-1, 4-phenylene oxide
S(PPO)	Homopolymer of DMP synthesized in laboratory
C(PPO)	Commercially available PPO
Co-A	Copolymer-A with DMP:DPP molar ratio 90 : 10
Co-B	Copolymer-B with DMP:DPP molar ratio 75 : 25

Co-C	Copolymer-C with DMP:DPP molar ratio 65 : 35
PDPPO	Poly(2,6-diphenyl-1,4-phenyleneoxide)
Permeability units	Barrers, in SI units 1 Barrer = $7.5005 \times 10^{-18} \text{ m}^2 \text{ s}^{-1} \text{ Pa}^{-1}$
n-Pentane	<i>n</i> -C ₅ H ₁₂ hydrocarbon
PDMS	Poly(dimethyl siloxane)
PAAM	Poly(acryl amide)
PVDF	Poly(vinylidene difluoride)
PAEK	Poly(aryl ether ketone)
Azide	2,6-bis(4-azidobenzylidene)-4methyl- cyclohexanone
TEG	Triethylene glycol
FFV	Fractional free volume

REFERENCES

- Baker, R. W. *Ind. Chem. Res.* **2002**, *41*, 1393.
- Semenova, S. L. *J. Membr. Sci.* **2004**, *231*, 189.
- Tanaka, K.; Taguchi, A.; Hao, J.; Kita, H.; Okamoto, K. *J. Membr. Sci.* **1996**, *121*, 197.
- Ito, A.; Hwang, S. *J. Appl. Polym. Sci.* **1989**, *38*, 483.
- Park, Y. S.; Won, J.; Kang, Y. S. *J. Membr. Sci.* **2001**, *183*, 163.
- Ravanchi, M. T.; Kaghachi, B. T.; Kargari, A. *Chem. Eng. Process. Process. Intensification* **2010**, *49*, 235.
- Chilukuri, P.; Rademakers, K.; Nymeijer, K.; van der Ham, L.; van den Berg, H. *Ind. Eng. Chem. Res.* **2007**, *46*, 8701.
- Duan, S.; Ito, A.; Ohkawa, A. *J. Membr. Sci.* **2003**, *215*, 53.
- Chng, M. L.; Xiao, Y.; Chung, T.; Toriida, M.; Tamai, S. *Carbon* **2009**, *47*, 1857.
- Kim, H.; Kim, H. G.; Kim, S.; Hum, S. S. *J. Membr. Sci.* **2009**, *344*, 211.
- Giannakopoulos, I. G.; Nikolakis, V. *Ind. Eng. Chem. Res.* **2005**, *44*, 226.
- Susheela, B.; Sridhar, S.; Khan, A. A. *J. Membr. Sci.* **1998**, *147*, 131.
- Ilinich, O. M.; Lapkin, A. A. *Polymer* **2002**, *43*, 3209.
- Khulbe, K. C.; Matsuura, T.; Noh, S. H. *J. Membr. Sci.* **1998**, *145*, 243.
- Katz, R.; Munk, B. F. *J. Oil Color Chem. Assoc.* **1969**, *52*, 418.
- Zubov, P. I.; Voronkov, V. A.; Sukharev, L. A. *Vysokomol. Soedin. Ser. B* **1968**, *10*, 92.
- Mark, J. E.; Eisenberg, A.; Graessley, W.; Mandelkern, L.; Samulski, E. T.; Koenig, J. L. *Physical Properties of Polymers*, ACS Series, 2nd ed.; American Chemical Society, Washington, **1993**; Chapter 2.
- Susheela, B.; Sridhar, S.; Khan, A. A. *J. Membr. Sci.*, **2000**, *67*, 174.
- Mark, H. F.; Bikales, N. M.; Overberger, C. G.; Menges, G. *Encyclopedia of Polymer Science and Engineering*, 2nd ed.; Wiley Interscience Publications: New York, **1976**; Vol. 13.
- Brandrup, J.; Immergut, E. H. *Polymer Handbook*; Wiley Interscience Publications: New York, **1974**, Chapter 4.
- Alfeeli, B.; Jain, V.; Johnson, R. K.; Beyer, F. L.; Heflin, J. R.; Agah, M. *Microchem. J.* **2011**, *98*, 240.
- Alentiev, A. Y.; Yampolskii, Y. P.; Shantarovich, V. P.; Nemsler, S. M.; Plate, N. A. *J. Membr. Sci.* **1997**, *126*, 123.
- Vankrevelen, D. W. *Properties of Polymers: Their Correlation with Chemical Structure*, 3rd ed.; Elsevier: Amsterdam, **1990**.
- Marathe, S.; Mohandas, T. P.; Sivaram, S. *Macromolecules* **1995**, *28*, 7318.
- Lapkin, A. A.; Roschupkina, O. P.; Ilinich, O. M. *J. Membr. Sci.* **1998**, *141*, 223.
- Hensema, E. R.; Mulder, M. H. V.; Smolder, C. A. *J. Appl. Polym. Sci.* **1993**, *49*, 2081.
- Ilinich, O. M.; Semin, G. L.; Chertova, M. V.; Zamarev, K. J. *J. Membr. Sci.* **1992**, *66*, 1.
- Ilinich, O. M.; Zamarev, K. J. *J. Membr. Sci.* **1993**, *82*, 149.
- Jansen, J. C.; Macchione, M.; Raharjo, R.; Freeman, B. D.; Drioli, E. *Desalination* **2006**, *199*, 461.